ROCK SLOPE STABILITY ANALYSIS FOR THE SEVEN CATARACTS VISTA ROAD CUT OF THE MT. LEMMON HIGHWAY, TUCSON, ARIZONA

by

Pinnaduwa H. S. W. Kulatilake[2], Jeongi-Gi Um[3], Greg Crum[4] and Graham Irvine[4]

Abstract. The seven cataracts Vista road cut is located eight miles up the Mt. Lemmon Highway northeast of Tucson, Arizona. The rock mass in the area has a number of discontinuities that produce a potentially unstable slope, as the present cut slope is approximately 90° in most of the area. The purpose of this study was to determine the stability of the road cut. Field data were collected on discontinuity geometry using scanline surveys. Also rock joints and intact rock samples were obtained from the field to perform laboratory tests to determine basic rock joint properties as well as routine intact rock properties. Discontinuity geometry data were analyzed to estimate important discontinuity geometry parameters to perform rock slope kinematic and block theory analyses. The results support in-field observations of a potentially unstable slope. The block theory analysis resulted in the identification of eight key blocks, of which the lowest maximum safe slope angle was 27°. Many potential key blocks were also identified. The results from the kinematic analysis support the existence of the key blocks determined by the block theory analysis. The purpose of the maximum safe slope angles for the key blocks is not to suggest the reduction of the current slope angle. Rather they are to show that instabilities exist and that external support may be needed in some places to prevent a major failure. The potential key blocks could become hazardous under external forces. Further analyses of the seven Cataracts Vista road cut will need to look into the effects of external forces, such as water forces and earthquake forces. Also, the key blocks and the potential key blocks that were found in general through the block theory analysis should be physically found in the field before final conclusions about the stability of the site can be drawn.

Additional Key Words: rock mass stability, discontinuities, discontinuity geometry, discontinuity shear strength

Introduction

The Seven Cataracts Vista road cut is located approximately 8 miles up the Mt. Lemmon Highway, northeast of Tucson, Arizona. The road up to this point has recently undergone improvements, including widening, to provide visitors with a safer drive up the mountain. At the Seven Cataracts Vista pullout, a significant amount of widening has taken place. The road cut face is 6 - 17 m high in the vicinity of the vista point. The road makes a 90° turn as it reaches the pullout then heads across a newly constructed bridge and continues up the mountain. A map of the area can be seen in Fig. 1. The Seven Cataracts area is of particular concern because of the existence of a high number of discontinuities in the area, as well as the extremely high cut slope angle. The angle for the majority of the rock face is approximately 90° with some areas being overhung. On visual observation alone, it is apparent that the slope is somewhat unstable. There are a number of prominent joint sets in the area, which create visible blocks. Debris from minor to large block failures finds its way onto the shoulder of the road, and sometimes onto the roadway itself. The purpose of this study has been to ascertain if the cut slope in the vicinity of the Seven Cataracts Vista is dangerously unstable, and if it needs to be decreased to prevent dangerous failure. The Mt. Lemmon Highway is a highly traveled road, and a substantial failure could have drastic ramifications.

The road cut has been made through mylonitic Catalina gneiss (mylonite). Mylonite is the result of the metamorphosis of granite and is typically highly

1. Paper presented at the 1996 National meeting of the American Society for Surface Mining and Reclamation, Scottsdale, Arizona, August 13-19, 1999
2. Professor, Department of Mining and Geological Engineering, University of Arizona, Tucson AZ 85721
3. Senior Research Specialist, Department of Mining and Geological Engineering, University of Arizona, Tucson AZ 85721
4. Undergraduate Student, Department of Mining and Geological Engineering, University of Arizona, Tucson AZ 85721

Proceedings America Society of Mining and Reclamation, 1999 pp 393-407
DOI: 10.21000/JASMR99010393

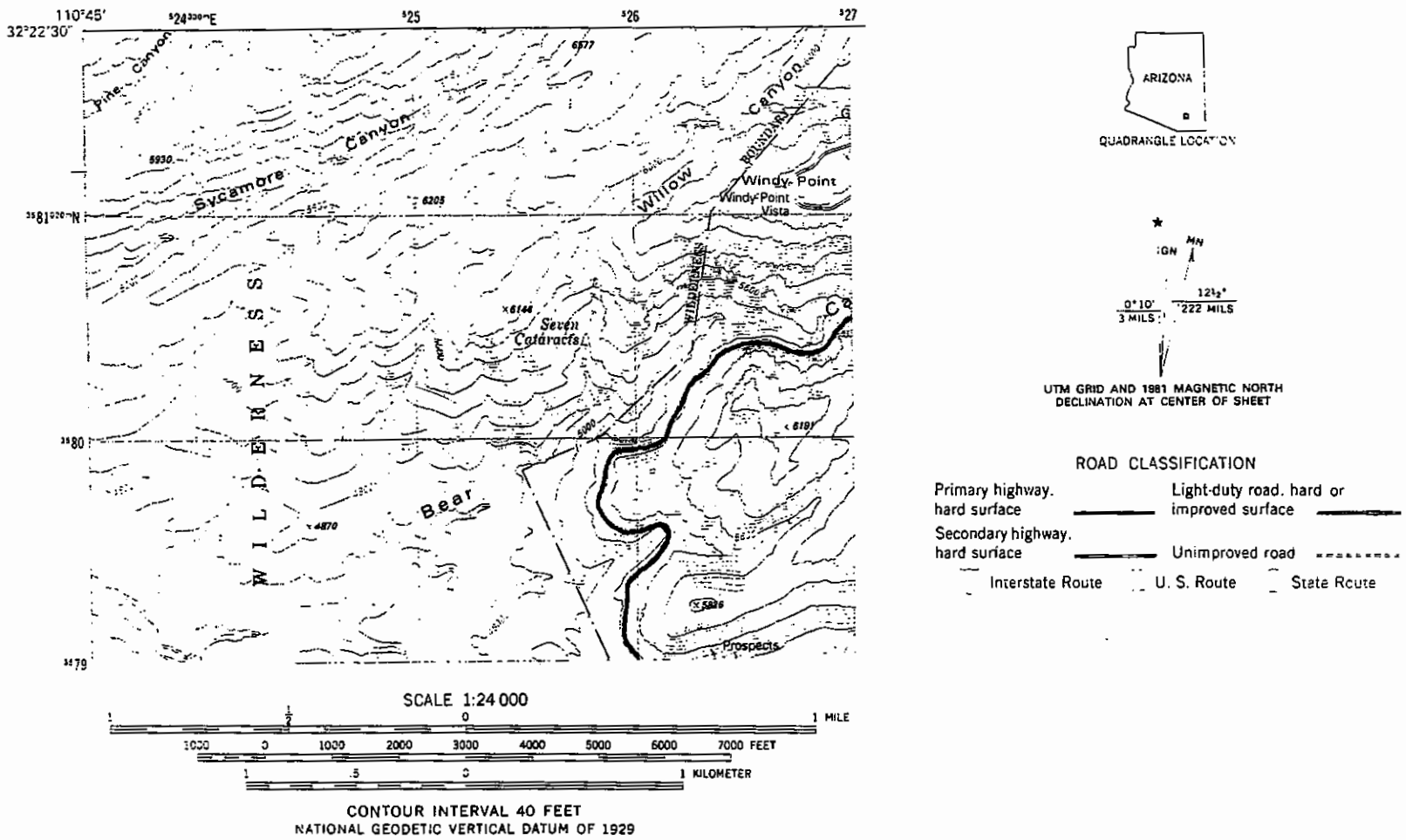

Figure 1. Map of the Seven Cataracts Vista area.

foliated. The mylonite in this area is also highly weathered in places, which may effect its overall strength. Sections of the road cut have a high density of joints as well as exceedingly weathered rock. Still, there are a few places along the road cut that are composed of very competent rock with a low discontinuity frequency. The aim of this study is to identify and determine the degree of slope instability in the area.

The examination of the Seven Cataracts road cut was broken into three major sections. The first is the data collection segment. This portion of the study was performed in the field and was composed of the collection of joint orientation data for a selected portion of the road cut, as well as the collection of intact rock and joint samples for further testing. The second step in the analysis was to obtain the rock properties of the mylonite, which the cut slope was formed in. The property that was most crucial was the friction angle of discontinuities. The next portion of the study was data analysis. Kinematic and block theory analyses were applied to examine the stability of the road cut. The final portion of this study was the compiling of the results from the various methods implemented.

Data Collection

The data collection took place at the site and consisted of the collection of discontinuity orientations, as well as the collection of rock samples for rock property analysis.

Scanline Surveys

To collect the joint orientation data, the cut slope face was broken down into a number of scanlines. Horizontal and vertical scanlines were utilized in collecting joint orientation data for the area. The vertical scanline was primarily used to record the horizontal joints in an area, where as the horizontal scanline included the rest of the discontinuities. All of the data collected in the field was recorded on scanline survey logging forms.

For the horizontal scanlines, a section of the face was measured off with a metric measuring tape laid on the ground. The height of the face was estimated with the help of a scaled staff 6.5 meters tall. The boundaries of the scanline were set as the top of the rock face, which was recorded as the cut-off length on the logging form. The horizontal boundary of the scanline was set according to the length of the straight face. As noted before, the rock face completes a 90° turn. To avoid bending the scanline, the curve of the cut slope was approximated with the ten straight sections, named correspondingly Sections 1, 2, 3, ... ,10. The starting reference point is at the west end of the southern most guard rail of the bridge. Section 1 starts at this reference point. The surveyed region extends down the Mt. Lemmon Highway, in a westerly to southerly direction. After section 1, a 54m gap was left before the initiation of Section 2. The following are the bounds to each section with respect to the reference point:
Section 1: 0 –11m, Section 2: 65m – 85m, Section 3: 85m – 105m, Section 4: 105m – 135m, Section 5: 135m – 161m, Section 6: 161m – 187m, Section 7: 187m – 213m, Section 8: 213m – 236m, Section 9: 236m – 259m, Section 10: 259m – 284m.

After the scanline area was set, the collection of orientation data could commence. The overall dip direction and dip of the face was measured. Individual joints within the scanline were identified and were projected out from the rock face until they intersected the scanline. This distance from the beginning of the scanline was recorded as the intersection distance. Strike and dip measurements were taken to identify the orientation of each discontinuity. Strike measurements were made with respect to the "right hand rule"; i.e. the direction of the strike is to the right when a plane dips towards the viewer.

Vertical scanlines were conducted to measure the orientations of the horizontal joints. Three to four vertical scanlines were performed for each horizontal section using a scaled staff to measure intersection distances. The majority of the orientation data recorded for the vertical lines was identical to the horizontal lines.

Rock Sampling

Samples of rock were collected from the site for further testing in the lab. Only samples that were representative of the cut slope rock were picked for testing. Cores of these rock samples were drilled out and a number of tests were conducted on them, these tests will be discussed further in the Rock Properties Testing section. Not only were continuous rock samples collected, but rock joints were also collected to perform direct shear tests on. Care was taken to ensure that the orientation of the joints was known before they were removed from the face. This helped guarantee that the joint was tested in the correct direction and from the correct seating position.

Joint Orientation Analysis

One of the computer programs in FRACNTWK software (Kulatilake et al., 1998) was used to find the number of discontinuity sets in the investigated rock mass. Two steep discontinuity sets and one shallow discontinuity set was found to exist (Fig. 2) in the Seven Cataracts Vista Area,

Basic Mechanical Properties of Intact Rock and Rock Joints

Brazilian and uniaxial compressive tests were performed to estimate basic mechanical properties of intact rock (mylonitic Catalina gneiss). These tests were performed according to ASTM standard procedures. Brazilian tension tests gave a mean tensile strength of 17.9 MPa with a standard deviation of 3.0. Mean uniaxial strength was found to be 94.8 MPa with a standard deviation of 6.4. Tests produced a mean Young's modulus of 19.5 GPa and a mean Poisson's ratio of 0.36.

Direct shear tests were performed on four different samples - one large-scale (6.0 in. square) and three small-scale (2.5 in. square). All samples were taken from existing joints except one saw-cut, which was used to obtain a basic friction angle, ϕ_b. Samples were trimmed and prepared for use in the Wykeham Farrance 25302 direct shear machine, for small-scale (4 in. square box), and the Wykeham Farrance 25502 direct shear machine, for large-scale (12 in. square box). Small-scale samples were cast in hydrostone and the large-scale sample was cast in concrete. The tests were preformed using 4 different normal stresses: 25 psi, 50 psi, 100 psi, and 200 psi for the small scale, and 50 psi, 100 psi, 200 psi and 400 psi for the large scale to estimate the shear strength of joints. Direct shear tests produced a basic friction angle of 25° for the smooth mylonite joints. For the natural rough mylonite joints, a mean friction angle of 37° with a standard deviation of 1.4 was obtained.

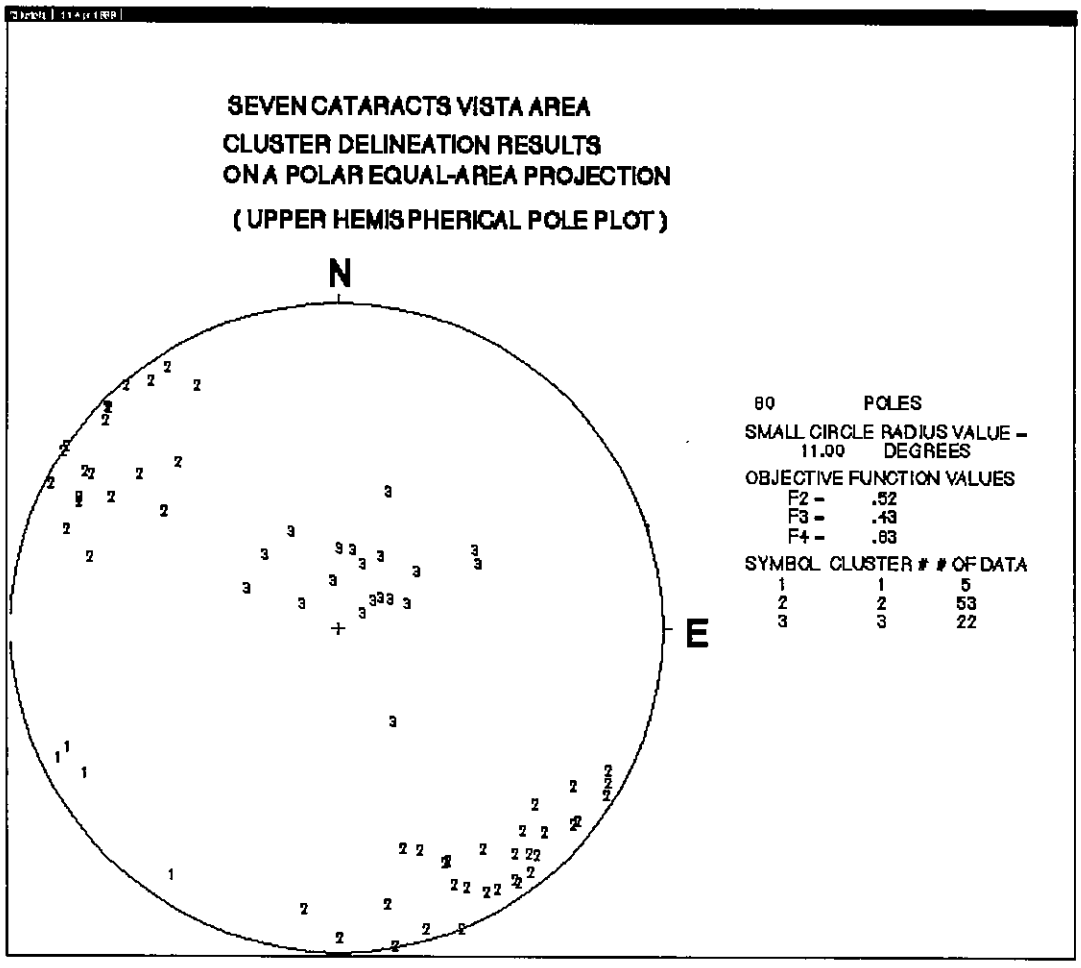

Figure 2. Discontinuity sets in Seven Cataracts Vista area.

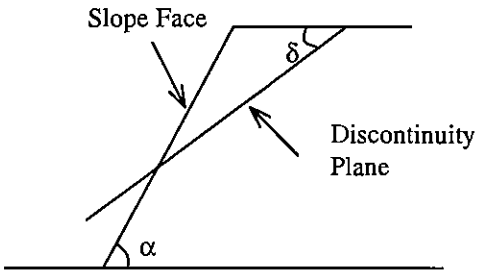

Sliding requires $\alpha > \delta$

(a)

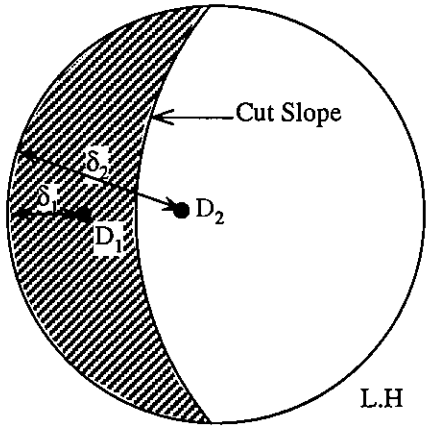

D_i: dip vector of discontinuity plane i
D_1 allows sliding
D_2 does not allow sliding

(b)

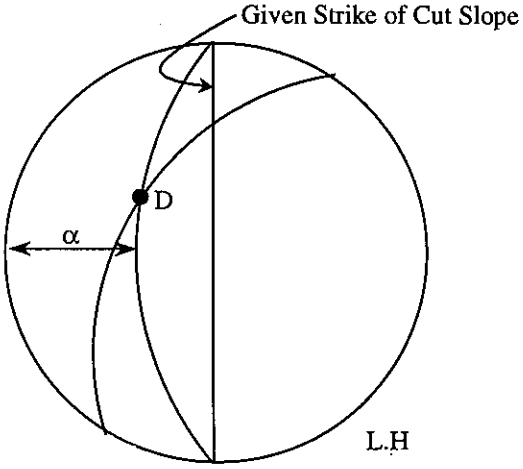

D: dip vector of the discontinuity plane
α: maximum safe cut slope angle

(c)

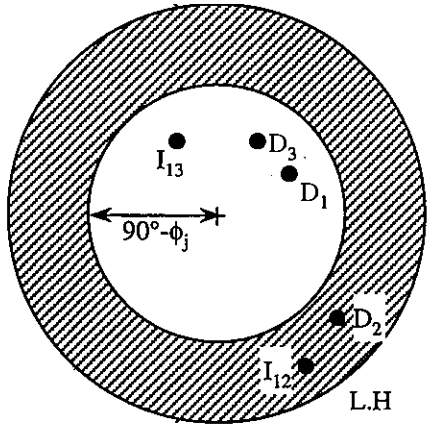

Maximum safe cut slope angle corresponding to D_2 &I_{12} is 90°.
Use construction given in Fig. 3(c) to estimate maximum safe cut slope angles corresponding to D_1, D_3 &I_{13}

(d)

Figure 3. Concepts related to kinematic analysis for plane sliding (Goodman(1989)) (a) daylighting requirements on a pictorial diagram. (b) daylighting requirements on a streographic plot. (c) great circle for cut slope providing the maximum safe slope angle. (d) influence of ϕ_j on maximum safe cut slope angle

Kinematic Analyses

"Kinematic" refers to the motion of bodies without reference to the forces that cause them to move (Goodman 1989). Kinematic analyses are very useful to investigate possible failure of rock masses which contain discontinuities. Failure involving movement of rock blocks on discontinuities combine one or more of the three basic modes-plane sliding, wedge sliding and toppling. For the Catalina Highway, kinematic analyses were performed to estimate maximum safe slope angles with respect to the aforementioned three basic failure modes. The basic concepts related to estimation of maximum safe slope angles for the three basic modes of failure are briefly explained below.

Theory

Plane Sliding. Consider the case of plane sliding under gravity alone as shown in Fig. 3(a). Any block tending to slide on a single plane surface will translate down the slope parallel to the dip of the discontinuity. If a cut slope is inclined at an angle α to the horizontal, the conditions for a plane slide are that the dip vector of the discontinuity, **D**, be pointed into the free space of the excavation and plunge at an angle less than α. If δ is greater than α, the block will be stable and no sliding will take place.

This concept can be represented on the stereographic projection (Fig. 3(b)). The cut slope can be constructed as a great circle in the lower hemisphere. $\mathbf{D}_1$ is the dip vector of discontinuity plane 1, and $\mathbf{D}_2$ is the dip vector of discontinuity plane 2. δ_1 and δ_2 are dip angles of planes 1 and 2, respectively. In this example, δ_1 is less than α, and therefore, plane 1 would allow a plane slide. On the other hand, δ_2 is greater than α and plane 2 would not allow a plane slide. In other words, if the dip vector of the discontinuity plane lies in the shaded region, then the plane would allow a slide. The limiting situation arises when the great circle of the cut slope passes through the dip vector of the discontinuity plane. When this occurs, the dip angle of the cut slope corresponds to the maximum safe slope angle with respect to plane sliding.

Figure 3(c) shows the reverse situation. If the dip vector of a discontinuity surface is known, it is possible to determine the maximum safe slope angle corresponding to a cut of assigned strike. The maximum safe slope angle α is the dip of the great circle passing through the given strike and the known dip vector **D**.

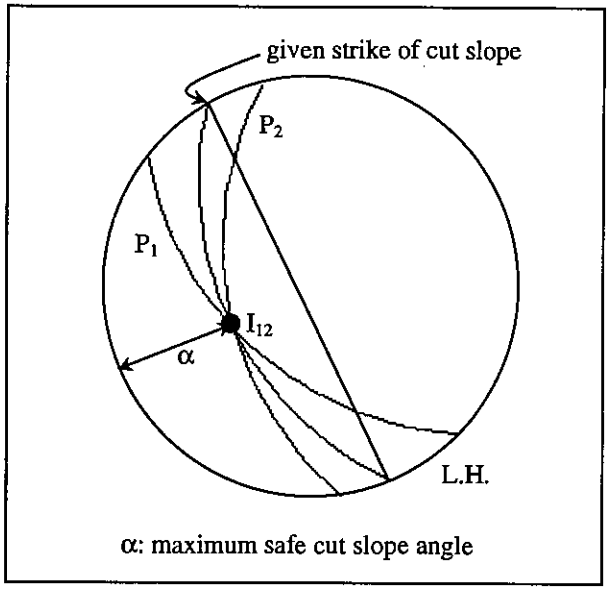

Figure 4. Stereographic construction to obtain the maximum safe slope angle for wedge sliding.

It is important to note that in the case of plane sliding under self weight alone, failure can occur only if the surface of sliding dips steeper than ϕ_j. Therefore, in a lower hemispherical stereographic projection, if a dip vector D of a discontinuity lies in the shaded area in Fig. 3(d), plane sliding will not occur under any cut slope angle. That means the corresponding maximum safe cut slope angle is 90°. Thus, it is necessary to use the concepts shown in both Figs. 3(c) and (d) in estimating the maximum safe cut slope angles under the plane sliding situation.

Wedge Sliding. Sliding along a line of intersection occurs when two discontinuity planes intersect to make a wedge. Figure 4 shows how to obtain graphically the maximum safe cut slope angle for a possible sliding wedge. When discontinuity planes 1 (P_1) and 2 (P_2) make a wedge, the maximum safe slope angle for a cut slope of assigned strike can be found in a similar way to the plane sliding case. If the cut is made with the strike as shown in the figure, the maximum safe slope angle α is obtained by the dip of the great circle which passes through the intersection of planes 1 and 2 (I_{12}) and the points corresponding to the assigned strike.

Note that Fig. 3(d) is equally applicable for wedge sliding situation. If the line of intersection of two discontinuity planes, I_{ij} lie in the shaded area in Fig. 3(d), then the maximum safe cut slope angle corresponding to I_{ij} is 90°. Thus, the concepts shown in Figs. 3(d) and 4 should be used in estimating maximum safe cut slope angles under wedge sliding situation.

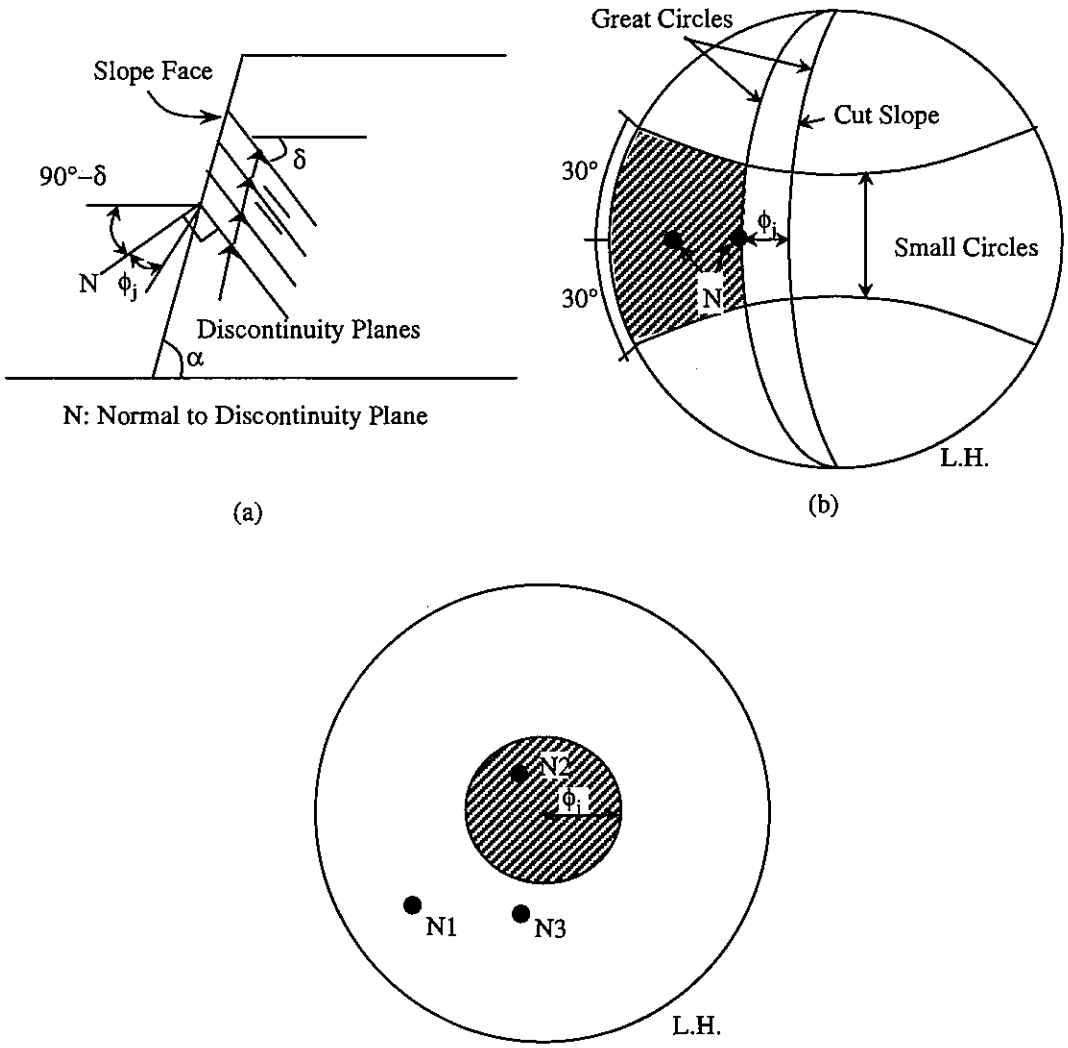

* Maximum safe cut slope angle corresponding to N2 is 90° .
* Use construction given in Fig 5(b) to estimate maximum safe cut slope angles corresponding to N1 & N3.

Figure 5. Concepts related to kinematic analysis for toppling (Goodman(1989)) (a) pictorial diagram. (b) on a streographic plot. (c) influence of ϕ_j on maximum safe cut slope angle

Toppling. Fig. 5 illustrates the kinematic analysis for toppling under gravity alone. Toppling can occur only if the discontinuities strike nearly parallel to the strike of the slope, say within 30°. In addition, discontinuity spacing should be low as shown in Fig. 5(a) to form thin layers of rock. For toppling failure, first it is necessary to initiate interlayer slip before large flexural deformations take place within the layers. If the layers have angle of friction ϕ_j, slip will occur only if the direction of applied compression (which is along the dip vector of slope) makes an angle greater than ϕ_j with the normal to the layers. If the cut slope is inclined α to the horizontal and the dip of discontinuity planes is δ, then the kinematic requirement for toppling is $(90-\delta) + \phi_j < \alpha$ as shown in Fig. 5(a). On a lower hemispherical stereographic projection, for toppling failure to occur, the normal vector **N** of the discontinuity should lie within the shaded area as shown in Fig. 5(b). The situation corresponding to the maximum safe cut slope angle occurs when **N** falls on the great circle which is ϕ_j degrees below the cut slope and striking parallel to it. Note that when **N** lies outside the two small circles shown in Fig. 5(b), the corresponding maximum safe cut slope angle is 90°. Also, it is important to note that toppling can occur only on discontinuities whose normals plunge at an angle less than $90-\phi_j$. That means with respect to the lower hemispherical stereographic plot shown in Fig. 5(c), if a normal vector of a discontinuity lies within the shaded area shown in Fig. 5(c), then the corresponding maximum safe cut slope angle is 90°. Thus, the concepts shown in both Figs. 5(b) and 5(c) should be used in estimating the maximum safe slope angles for toppling mode. Also, it is important to check whether the discontinuity geometry produces thin rock layers as shown in Fig. 5(a).

Analysis Results

Kinematic analyses were conducted using major discontinuities. In the context of this study, a major discontinuity is defined as any discontinuity that is of continuous extent throughout a given section. Major discontinuities were selected on the basis to provide a representative sampling of the joint sets observed in each section. In order to limit the number of wedge sliding possibilities, given by $n(n-1)/2$, where n is the number of major discontinuities having different orientations in the section, many of the sections were further divided into subsections denoted by a lower case letter following the section number, e.g. 2a. These subsections do not represent actual measured segments of a section. They merely represent another possible combination of the observed major discontinuities. Parallel discontinuities were also excluded from these analyses. To be on the conservative side, the basic friction angle value was used to represent the peak shear strength of mylonite joints.

A computer code called KINEM, developed by Kulatilake and Chen Jianping (Um et al. 1996), was used to determine maximum safe slope angles (MSA) for each of the 10 sections mentioned in the "Data Collection" section. The results from this program represent maximum safe slope angles for discontinuities of continuous extent that actually exist in the same general vicinity, and are exposed on the surface of the cut slope and intersect one another if their orientations are not parallel. The results are addressed according to the failure mode. The maximum safe slope angles for all the sections are shown in Table 1. It seems that sections 3a and 4b can have MSA of 90°. For all other sections, MSA is less than 90° and for some sections it can be low as 25°. It is important to note that the MSA for a section is determined by the lowest MSA value obtained for the section.

Block Theory Analysis

The principal idea behind block theory analysis is that it allows many different combinations of discontinuities to be passed over and to directly identify and consider critical rock blocks known as "key blocks". Fig. 6 shows five types of blocks in a surface excavation formed by discontinuities. Types of blocks can be divided into infinite and finite blocks. An infinite block(type V), as shown in Fig. 6(a) is not dangerous as long as it is incapable of internal cracking. Finite blocks can be categorized into nonremovable and removable blocks. Fig. 6(b) is an example of type IV nonremovable tapered blocks. It is finite, but it can not come out to free space because of its tapered shape. Finite and removable blocks can be separated into three categories, namely type III, type II, and type I, and identification of these blocks plays an important role in rock slope design. As shown in Fig. 6(c), a type III block is stable without friction under its gravity alone. A type II block which is in Fig. 6(d) can be remained stable as long as the sliding force of the block is less than its frictional resistance. Under only gravitational loading, the type II blocks are stable. However, it can come out into the free surface of excavation if there are external forces like water forces, inertia forces etc. that make the total sliding force to be greater than the frictional resistance. Therefore, type II blocks are also called potential key blocks. Finally, a key block which is denoted by type I shown in Fig. 6(e) can slide into free space under gravitational loading without any external force unless a proper support system is provided. Therefore, the identification of key blocks is

Table 1. Maximum safe slope angles (MSA) from kinematic analysis on selected major discontinuities

Section 1 Dip Dir of Cut Slope =4°	Discontinuity (D/DD)	PS-MSA	Top-MSA
	1 (75°/156°)	90°	42°
	2 (89°/319°)	89°	90°
	3 (77°/290°)	86°	90°
	4 (20°/360°)	90°	90°
	Wedge Sliding Discon.	Plunge/Trend	WS-MSA
	1, 2	46°/230°	90°
	1, 3	57°/221°	90°
	1, 4	08°/068°	90°
	2, 3	66°/231°	90°
	2, 4	13°/049°	90°
	3, 4	19°/015°	90°
Section 2a Dip Dir of Cut Slope =357°	Discontinuity (D/DD)	PS-MSA	Top-MSA
	1 (85°/327°)	86°	90°
	2 (83°/130°)	90°	90°
	3 (21°/030°)	90°	90°
	4 (70°/147°)	90°	48°
	5 (75°/170°)	90°	40°
	Wedge Sliding Discon.	Plunge/Trend	WS-MSA
	1, 2	55°/050°	67°
	1, 3	19°/055°	90°
	1, 4	00°/057°	90°
	1, 5	48°/243°	90°
	2, 3	21°/043°	90°
	2, 4	50°/212°	90°
	2, 5	73°/196°	90°
	3, 4	18°/064°	90°
	3, 5	13°/084°	90°
	4, 5	68°/122°	90°
Section 2b Dip Dir of Cut Slope =357°	Discontinuity (D/DD)	PS-MSA	Top-MSA
	1 (85°/312°)	86°	90°
	2 (83°/118°)	90°	90°
	3 (13°/053°)	90°	90°
	4 (89°/170°)	90°	26°
	Wedge Sliding Discon.	Plunge/Trend	WS-MSA
	1, 2	49°/036°	56°
	1, 3	13°/041°	90°
	1, 4	81°/254°	90°
	2, 3	12°/029°	90°
	2, 4	82°/087°	90°
	3, 4	12°/080°	90°
Section 2c Dip Dir of Cut Slope =357°	Discontinuity (D/DD)	PS-MSA	Top-MSA
	1 (88°/297°)	89°	90°
	2 (85°/120°)	90°	90°
	3 (15°/060°)	90°	90°
	4 (85°/180°)	90°	30°
	Wedge Sliding Discon.	Plunge/Trend	WS-MSA
	1, 2	23°/208°	90°
	1, 3	13°/027°	90°
	1, 4	85°/004°	90°
	2, 3	13°/031°	90°
	2, 4	80°/060°	90°
	3, 4	13°/089°	90°
Section 3a Dip Dir of Cut Slope =6°	Discontinuity (D/DD)	PS-MSA	Top-MSA
	1 (78°/297°)	86°	90°
	2 (80°/302°)	86°	90°
	3 (25°/294°)	56°	90°
	4 (17°/020°)	90°	90°
	Wedge Sliding Discon.	Plunge/Trend	WS-MSA
	1, 2	65°/235°	90°
	1, 3	02°/207°	90°
	1, 4	17°/023°	90°

Section 3a	Wedge Sliding Discon.	Plunge/Trend	WS-MSA
	2, 3	04°/213°	90°
	2, 4	17°/029°	90°
	3, 4	15°/350°	90°
Section 3b Dip Dir of Cut Slope =6°	Discontinuity (D/DD)	PS-MSA	Top-MSA
	1 (88°/314°)	89°	90°
	2 (68°/286°)	86°	90°
	3 (77°/296°)	85°	90°
	4 (81°/214°)	90°	35°
	Wedge Sliding Discon.	Plunge/Trend	WS-MSA
	1, 2	51°/227°	90°
	1, 3	57°/227°	90°
	1, 4	80°/236°	90°
	2, 3	44°/219°	90°
	2, 4	68°/281°	88°
	3, 4	75°/267°	90°
Section 4a Dip Dir of Cut Slope =0°	Discontinuity (D/DD)	PS-MSA	Top-MSA
	1 (60°/316°)	67°	90°
	2 (68°/156°)	90°	49°
	3 (90°/303°)	90°	90°
	4 (82°/139°)	90°	90°
	5 (18°/070°)	44°	90°
	Wedge Sliding Discon	Plunge/Trend	WS-MSA
	1, 2	19°/238°	90°
	1, 3	21°/033°	90°
	1, 4	04°/228°	90°
	1, 5	15°/037°	90°
	2, 3	53°/213°	90°
	2, 4	47°/220°	90°
	2, 5	18°/074°	49°
	3, 4	63°/213°	90°
	3, 5	15°/033°	90°
	4, 5	17°/051°	90°
Section 4b Dip Dir of Cut Slope =0°	Discontinuity (D/DD)	PS-MSA	Top-MSA
	1 (66°/308°)	75°	90°
	2 (90°/304°)	90°	90°
	3 (11°/303°)	90°	90°
	4 (84°/129°)	90°	90°
	Wedge Sliding Discon.	Plunge/Trend	WS-MSA
	1, 2	09°/034°	90°
	1, 3	01°/218°	90°
	1, 4	02°/219°	90°
	2, 3	00°/214°	90°
	2, 4	39°/214°	90°
	3, 4	01°/219°	90°
Section 5a Dip Dir of Cut Slope =336°	Discontinuity (D/DD)	PS-MSA	Top-MSA
	1 (90°/072°)	90°	90°
	2 (86°/164°)	90°	29°
	3 (27°/334°)	27°	90°
	4 (37°/020°)	46°	90°
	Wedge Sliding Discon.	Plunge/Trend	WS-MSA
	1, 2	86°/162°	90°
	1, 3	75°/162°	90°
	1, 4	75°/162°	90°
	2, 3	05°/254°	90°
	2, 4	23°/076°	90°
	3, 4	27°/333°	27
Section 5b Dip Dir of Cut Slope =336°	Discontinuity (D/DD)	PS-MSA	Top-MSA
	1 (87°/122°)	90°	90°
	2 (80°/140°)	90°	35°
	3 (70°/132°)	90°	47°
	4 (37°/020°)	46°	90°

Section	Wedge Sliding Discon.	Plunge/Trend	WS-MSA
5b	1, 2	68°/205°	90°
Dip Dir of	1, 3	29°/210°	90°
Cut Slope	1, 4	36°/034°	54°
=336°	2, 3	36°/057°	78°
	2, 4	31°/056°	74°
	3, 4	32°/055°	73°
Section	Discontinuity (D/DD)	PS-MSA	Top-MSA
5c	1 (76°/124°)	90°	90°
Dip Dir of	2 (76°/187°)	90°	90°
Cut Slope	3 (37°/020°)	46°	90°
=336°	4 (78°/302°)	80°	90°
	Wedge Sliding Discon.	Plunge/Trend	WS-MSA
	1, 2	74°/156°	90°
	1, 3	35°/044°	61°
	1, 4	04°/213°	90°
	2, 3	08°/099°	90°
	2, 4	67°/242°	90°
	3, 4	37°/023°	48°
Section	Discontinuity (D/DD)	PS-MSA	Top-MSA
6	1 (80°/246°)	90°	90°
Dip Dir of	2 (73°/138°)	90°	43°
Cut Slope	3 (87°/314°)	87°	90°
=337°	4 (24°/054°)	90°	90°
	5 (26°/315°)	28°	90°
	Wedge Sliding Discon.	Plunge/Trend	WS-MSA
	1, 2	67°/181°	90°
	1, 3	80°/241°	90°
	1, 4	05°/335°	90°
	1, 5	25°/331°	25°
	2, 3	11°/225°	90°
	2, 4	24°/056°	90°
	2, 5	01°/228°	90°
	3, 4	24°/043°	90°
	3, 5	01°/044°	90°
	4, 5	17°/007°	90°
Section	Discontinuity (D/DD)	PS-MSA	Top-MSA
7	1 (79°/240°)	89°	90°
Dip Dir of	2 (69°/300°)	71°	90°
Cut Slope	3 (12°/354°)	90°	90°
=323°	4 (27°/150°)	90°	88°
	Wedge Sliding Discon.	Plunge/Trend	WS-MSA
	1, 2	69°/300°	71°
	1, 3	11°/328°	90°
	1, 4	27°/156°	90°
	2, 3	10°/026°	90°
	2, 4	12°/215°	90°
	3, 4	04°/067°	90°
Section	Discontinuity (D/DD)	PS-MSA	Top-MSA
8	1 (68°/155°)	90°	90°
Dip Dir of	2 (84°/245°)	86°	90°
Cut Slope	3 (77°/142°)	90°	90°
=288°	4 (07°/057°)	90°	90°
	Wedge Sliding Discon.	Plunge/Trend	WS-MSA
	1, 2	67°/170°	90°
	1, 3	50°/216°	76°
	1, 4	07°/068°	90°
	2, 3	74°/177°	90°
	2, 4	01°/335°	90°
	3, 4	07°/054°	90°
Section	Discontinuity (D/DD)	PS-MSA	Top-MSA
9a	1 (85°/142°)	90°	90°
	2 (90°/158°)	90°	90°
	3 (75°/330°)	85°	90°

Section	Discontinuity (D/DD)	PS-MSA	Top-MSA
9a	4 (40°/060°)	90°	76°
Dip Dir of	Wedge Sliding Discon.	Plunge/Trend	WS-MSA
Cut Slope	1, 2	72°/068°	90°
=260°	1, 3	21°/054°	90°
	1, 4	40°/056°	90°
	2, 3	75°/248°	75°
	2, 4	45°/068°	90°
	3, 4	39°/048°	90°
Section	Discontinuity (D/DD)	PS-MSA	Top-MSA
9b	1 (78°/154°)	90°	90°
Dip Dir of	2 (82°/151°)	90°	90°
Cut Slope	3 (85°/323°)	88°	90°
=260°	4 (39°/065°)	90°	77°
	Wedge Sliding Discon.	Plunge/Trend	WS-MSA
	1, 2	36°/235°	38°
	1, 3	33°/236°	35°
	1, 4	39°/074°	90°
	2, 3	31°/236°	34°
	2, 4	39°/068°	90°
	3, 4	38°/049°	90°
Section	Discontinuity (D/DD)	PS-MSA	Top-MSA
10a	1 (83°/149°)	90°	90°
Dip Dir of	2 (54°/304°)	63°	90°
Cut Slope	3 (62°/160°)	90°	90°
=259°	4 (11°/051°)	90°	90°
	Wedge Sliding Discon.	Plunge/Trend	WS-MSA
	1, 2	27°/235°	29°
	1, 3	25°/236°	90°
	1, 4	11°/060°	90°
	2, 3	26°/235°	28°
	2, 4	10°/027°	90°
	3, 4	10°/075°	90°
Section	Discontinuity (D/DD)	PS-MSA	Top-MSA
10b	1 (85°/145°)	90°	90°
Dip Dir of	2 (54°/304°)	63°	90°
Cut Slope	3 (60°/164°)	90°	90°
=259°	4 (20°/010°)	90°	90°
	Wedge Sliding Discon.	Plunge/Trend	WS-MSA
	1, 2	24°/233°	90°
	1, 3	33°/232°	36°
	1, 4	14°/056°	90°
	2, 3	28°/236°	30°
	2, 4	20°/019°	90°
	3, 4	08°/078°	90°
Section	Discontinuity (D/DD)	PS-MSA	Top-MSA
10c	1 (78°/135°)	90°	90°
Dip Dir of	2 (84°/145°)	90°	90°
Cut Slope	3 (54°/304°)	63°	90°
=259°	4 (60°/164°)	90°	90°
	5 (11°/051°)	90°	90°
	Wedge Sliding Discon.	Plunge/Trend	WS-MSA
	1, 2	58°/065°	90°
	1, 3	12°/223°	90°
	1, 4	50°/210°	61°
	1, 5	11°/047°	90°
	2, 3	23°/232°	90°
	2, 4	34°/231°	38°
	2, 5	11°/056°	90°
	3, 4	28°/236°	30°
	3, 5	10°/027°	90°
	4, 5	10°/080°	90°

PS: Plane sliding, Top: Toppling, WS: Wedge Sliding
MSA: Maximum Safe Slope Angle, (D/DD): (Dip/Dip Direction)

one of the most important parts in a rock slope stability analysis.

Stereographic Projection of a Discontinuity Plane

The stereographic projection is a strong tool for analysis of three dimensional structures such as rock block geometry. Fig. 7 shows the stereographic construction of a discontinuity plane on upper hemisphere. U_i and L_i denote the upper and lower half spaces of the discontinuity plane P_1, respectively, and its half spaces can be represented by binary digits. The number 0 corresponds to the symbol U_i, which is the half space above P_i and the number 1 corresponds to the symbol L_i which is the half space below P_1. In the upper hemisphere projection, the region above a discontinuity plane (U_i) is the area within the great circle of discontinuity plane P_i, and the region below the plane (L_i) is the area outside of its great circle as shown in Fig. 7.

The Finiteness and Removability of Blocks

Fig. 8 provides some terminology related to the representation of an excavation surface, on a stereonet. The rock mass side from an excavation surface is termed the Excavation Pyramid (EP) and it occupies the outside region of the great circle corresponding to the excavation surface on the stereonet. The free space region from an excavation is termed the Space Pyramid (SP) and it falls inside the great circle corresponding to the excavation surface. The spherical regions formed on the stereonet through the intersection of discontinuities are known as Joint Pyramids (JP). According to the finiteness theorem (Goodman and Shi 1985), a block is finite if it satisfies the criterion given below:

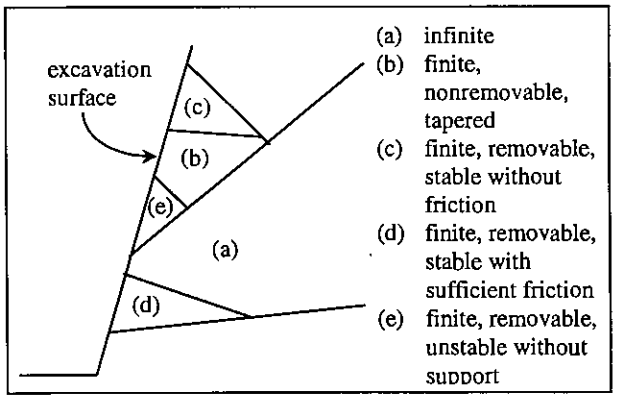

Figure 6. Key blocks in a surface cut. (a) infinite, (b) tapered, (c) stable, (d) potential key block, (e)key block.

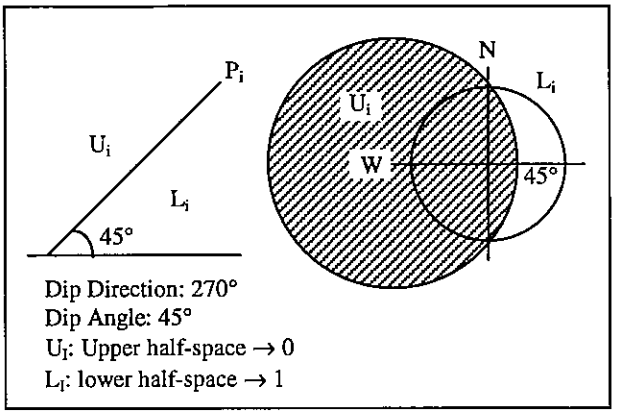

Figure 7. Stereographic construction of a discontinuity plane on upper hemisphere.

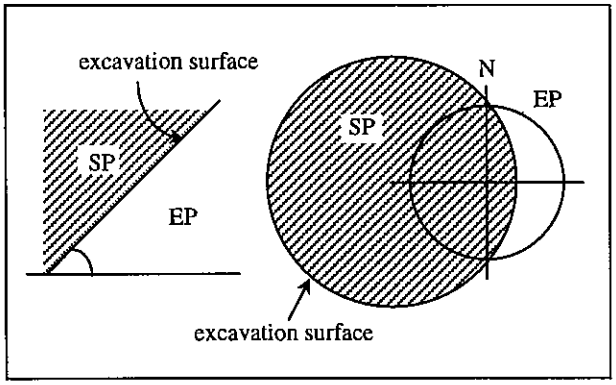

Figure 8. Stereographic construction of an excavation surface on upper hemisphere.

$$\text{Joint Pyramid(JP)} \subset \text{Space Pyramid(SP)} \quad (1)$$

The blocks which do not satisfy the criterion given above falls into the category of infinite blocks (type V). Therefore, by plotting discontinuity planes and the excavation surface on a stereonet and using the criterion given above, the finite blocks can be separated from the infinite blocks.

According to the removability theorem (Goodman and Shi 1985), for a block to be removable, in addition to satisfying the criterion given in Eqn. (1), the JP corresponding to the block should be non-empty. If JP is empty and the block satisfies the criterion given in Eqn. (1), the block belongs to the finite non-removable (tapered) category (type IV). Since JP is empty for finite tapered blocks, they do not show up on a stereographic projection. Therefore, the joint pyramids that satisfy the criterion given in Eqn. (1) on a stereographic projection belong to finite removable block categories (types I, II and III).

Separation Between Type I, II and III Blocks

Failure involving movement of rock blocks on discontinuities combine one or more of the following three basic modes; (a) lifting, (b) sliding on a single plane and (c) sliding on two planes. Only one joint pyramid exist for each of the above mentioned movement directions. A mode analysis (Goodman and Shi 1985, Chap. 9) can be performed to find JPs corresponding to all the movement directions. Type III blocks lack a movement mode. On the other hand, a movement mode can be found for each of the type I & II blocks. This concept allows separation of type III blocks from types I and II blocks.

Equilibrium equations given in chapter 9 of Goodman and Shi (1985) can be used to compute sliding forces, **F**, under the resultant active force, **r**, for the modes of lifting, single plane sliding and double plane sliding. A positive **F** corresponds to a type I block. Type II block produces a negative **F**. Um and Kulatilake (1996) have developed a computer code called SFORCE to perform this sliding force analysis.

Analysis Results

Block theory was applied to, the same major discontinuities that were used in kinematic analysis. Table 2 shows the MSA for all identified types I and II blocks. It is important to note that when the cut slope angle is less than MSA, both types I and II blocks become infinite (type V) blocks.

A total of eight type I blocks (keyblocks) were identified. These exist in sections 3, 5 and 7. MSA corresponding to type I blocks were found to be between 27° and 88°. Corresponding to a type I block, if it is needed to have a design slope angle greater than the MSA value calculated, then external rock support should be provided. Section 5 contains discontinuities that allow the formation of a total of six type I blocks. The minimum MSA of 27°, found in Section 5, was obtained for two different sliding modes: single plane sliding and double plane sliding. To calculate the required support, limit equilibrium analysis can be used incorporating the selected slope value, external forces acting on the block and the weight of the block.

Maximum safe slope angles are given in Table 2 for type II blocks (potential keyblocks) assuming that the resultant of weight of the block and external forces acting on the block exceeds the frictional resistance. Under these assumptions, type II blocks gave rise to many very low maximum safe slope angles, many in fact below the basic friction angle, ϕ_b, of 25° and one even at 1°. Corresponding to type II blocks, to have a design slope angle greater than MSA, it is necessary to perform a limit equilibrium analysis incorporating all the forces to evaluate whether external rock support is required. It is important to note that under only gravitational loading MSA corresponding to each type II block is 90 degrees. MSA values below the basic friction angle are only possible with type II blocks under external forces, and never with type I blocks.

The aim of the block theory analysis was to identify theoretically dangerous keyblocks (type I) and their corresponding maximum safe slope angles. Further studies will be needed to actually identify these keyblocks at the Seven Cataracts Vista site. Once these blocks have been identified, it will then be possible to look into the feasibility of providing them with external support.

As in the kinematic analyses, the maximum safe slope angles determined by use of block theory are for discontinuities of continuous extent that actually exist in the same general vicinity, that are exposed on the surface of the cut slope and intersect one another if their orientations are not parallel. This assumption is not always met. Discontinuities that intersect a scanline are assumed to exist throughout the rock mass in a given section. Subsections complicate matters even more, as these combinations of selected major discontinuities may not actually exist in the same general vicinity.

Comparison Between the Results of Kinematic and Block Theory Analyses

The kinematic and block theory analyses show similar results. Maximum safe slope angles for type I blocks correspond very well to the same sliding modes found in the kinematic analysis (Tables 1 and 2). Both methods show that the lowest maximum safe slope angle for type I blocks is 27°. For the type II blocks under gravitational loading, irrespective of the plunge angle of the dip vector (for single plane sliding) or the line of intersection (for the wedge mode) the sliding force due to gravity is less than the frictional resistance. Therefore, the MSA can be 90 degrees. According to the procedure used in the kinematic analysis, the dip vectors and lines of intersections having a plunge angle less than the friction angle produce maximum safe slope angles of 90 degrees. In the case of plane sliding under gravitational loading, the dip vectors having a plunge angle greater than the friction angle of the discontinuity do not produce type II blocks. However, in the case of

Table 2. Results of the block theory analysis on major discontinuities that included type I and II blocks. Maximum safe slope angles corresponding to type II blocks are based on the assumption that the resultant of weight of the block and external forces exceeds the available frictional resistance.

Segment	JP ⊂ SP	Sliding Mode	Type II Blocks	Type I Blocks	Sliding Force	Maximum Safe Slope Angle
1	1010	S_{34}	1010	---	---	19°
	1110	S_{24}	1110	---	---	19°
	0010	---	---	---	---	---
2a	00111	S_{12}	00111	---	---	67°
	10011	S_{13}	10011	---	---	40°
	00011	S_{23}	00011	---	---	34°
	10001	S_{34}	10001	---	---	76°
	01001	---	---	---	---	---
	00001	---	---	---	---	---
2b	0011	S_{12}	0011	---	---	57°
	1001	S_3	1001	---	---	17°
2c	0101	S_{13}	0101	---	---	14°
	1101	S_{23}	1101	---	---	16°
3a	1010	S_{14}	1010	---	---	18°
	0010	S_4	0010	---	---	18°
3b	0001	S_2	---	0001	0.75W	88°
4a	01111	S_{13}	01111	---	---	25°
	11110	S_{45}	11110	---	---	26°
	11100	S_5	11100	---	---	50°
	01110	S_{15}	01110	---	---	19°
	01100	---	---	---	---	---
	00110	---	---	---	---	---
4b	0111	S_{12}	0111	---	---	11°
5a	1110	S_{24}	1110	---	---	31°
	1100	S_3	---	1100	0.04W	27°
	1101	S_{34}	---	1101	0.02W	27°
5b	0110	S_{24}	---	0110	0.16W	73°
	0100	S_{34}	---	0100	0.02W	74°
	0101	S_{23}	0101	---	---	78°
5c	1101	S_{34}	---	1101	0.21W	48°
	1100	S_3	---	1100	0.23W	47°
6	11010	S_{15}	11010	---	---	25°
	11001	S_{34}	11001	---	---	47°
	11000	S_{45}	11000	---	---	19°
	11101	S_4	11101	---	---	78°
	11100	S_{35}	11100	---	---	2°
7	1001	S_3	1001	---	---	22°
	1011	S_2	---	1011	0.77W	70°
	0001	S_{13}	0001	---	---	10°
8	0011	S_{13}	0011	---	---	75°
	1010	S_{24}	1010	---	---	1°
	0010	---	---	---	---	---
9a	1000	---	---	---	---	---
	1001	S_{13}	1001	---	---	27°
9b	0101	S_{13}	0101	---	---	34°
	0001	S_{23}	0001	---	---	33°
10a	1001	S_{13}	1001	---	---	26°
	0001	S_{23}	0001	---	---	26°
	0011	S_{12}	0011	---	---	29°
10b	1001	S_{23}	1001	---	---	29°
	0001	S_{12}	0001	---	---	26°
	1101	S_{13}	1101	---	---	37°
10c	10000	---	---	---	---	---
	11001	S_{34}	11001	---	---	29°
	10001	S_{23}	10001	---	---	26°
	00001	S_{13}	00001	---	---	14°
	11101	S_{24}	11101	---	---	37°
	10101	S_{14}	10101	---	---	61°

wedge sliding under gravitational loading, it is possible to have type II blocks having the plunge of line of intersection exceeding both friction angles of the discontinuities forming the wedge. These blocks under kinematic analysis produce maximum safe slope angles less than 90 degrees. For these blocks it is not possible to make a comparison between the results obtained through kinematic and block theory analysis. For the rest of the type II blocks, the results agree between the two analyses. It is important to note that kinematic analysis produce maximum safe slope angles less than 90 degrees for type IV and V blocks. However, with respect to block theory analysis the maximum safe slope angle corresponding to types IV and V blocks can be considered as 90 degrees because they do not provide removable blocks. Block theory does not account for toppling failure, thus no comparison is possible.

The primary advantage of block theory over traditional kinematic analyses is that it gives the ability to theoretically identify the keyblocks that require immediate attention. It separates the most important and dangerous blocks from the less critical ones. However, without the ability to look into toppling failure, kinematic analysis should be performed in conjunction with block theory. In the case of this study, it should be noted that the most common mode of failure observed at the Seven Cataracts Vista site was toppling failure. Therefore, the maximum safe slope angles that correspond to toppling failure in the kinematic analysis should be taken into great consideration.

Both methods contain assumptions that lead to both conservative and non-conservative results. The assumption that all discontinuities of infinite extent leads to conservative results. Leaving many discontinuities out and not considering repeating joint sets, on the other hand, leads to non-conservative results. By far the criterion of most consequence is that, this study assumed only gravitational loading as the force which contributes to sliding. External forces, such as water forces and earthquake forces need to be considered in a further study. The slope stability analysis has confirmed the instabilities that were observed at the site. The results of both kinematic and block theory analyses show that under abiding conditions, the Seven Cataracts Vista road cut has and will experience failures.

Conclusions

The kinematic and block theory analyses have shown that instabilities exist in the Seven Cataracts Vista road cut. Eight key blocks (type I) were identified in the block theory analysis. Maximum safe slope angles for these key blocks (type I) ranged from 88° to as low as 27°. Numerous potential keyblocks were also identified. Maximum safe slope angles for these ranged from 78° to as low as 1° and show a strong potential for failures occurring under the influence of external forces, such as water forces and earthquake forces. The maximum safe slope angles from the kinematic analyses coincide very well with those for the type I blocks in the block theory. It is not possible to differentiate the types of blocks using the kinematic analysis. In addition, some conceptual differences exist between the kinematic and block theory analyses in estimating the maximum safe slope angles under gravitational loading. Therefore, a proper comparison cannot be made between the two analyses for block types II through V. For single and double plane sliding, block theory results are much superior to kinematic results. However, kinematic analysis is important in obtaining maximum safe slope angles under toppling mode.

The maximum safe slope angles presented here are not intended to suggest that present slope angles require lowering. The lowering of the present slope angle to accommodate these maximum safe slope angles is highly unfeasible. The amount of over burden needed to be removed to drastically lower the slope angle is unrealistic. These lower slope angles correspond to blocks or areas that may need external support. The lower slope angles for potential key blocks point out the hazard potentials that exist when external forces such as water and earthquake forces act on these slopes. This supports our observations during field data collection, which was conducted during this past winter's El Niño phenomena. Higher than normal precipitation was recorded in the Tucson area. This resulted in numerous minor to substantial rock slope failures that occurred on the Mt. Lemmon Highway.

In conclusion, this study has shown that the Seven Cataracts Vista road cut has regions that are currently unstable, and that other areas are marginally stable under normally dry conditions. Further studies looking into the effects of external forces other than gravitational loading, including water forces and earthquake forces, must be conducted to accurately determine their effects on the marginally stable type II blocks. An in-field study must also be conducted in order to physically locate type I blocks and to determine the feasibility of implementing external support.

References

Goodman, R.E. *Introduction to Rock Mechanics-2nd ed.* John Wiley & Sons, Inc., New York, 1989.

Goodman, R.E. and Shi, G.-H. *Block theory and Its Application to Rock Engineering*. Prentice-Hall, Inc., New Jersey, 1985.

Kulatilake, P.H.S.W. et al. Software manual for FRACNTWK- a computer package to model discontinuity geometry in rock masses, submitted to Metropolitan Water District of Southern California, 1998.

Um, J. and Kulatilake, P.H.S.W. Maximum Safe Slope Angles for Proposed Permanent Shiplock Slopes of the Three Gorges Dam Site in China Based on Application of Block Theory to Major Discontinuities. Proceedings of the 2nd North Amer. Rock Mech. Symposium, pp.529-536, Montréal, Québec, Canada, June 19-21, 1996.

Um, J., Kulatilake, P.H.S.W., Chen, J. and Teng, J. Maximum Safe Slope Angles for Proposed Shiplock of the Three Gorges Dam Site Based on Kinematic Analyses Performed on Major Discontinuities. Proceedings of the 13th Annual Meeting of ASSMR, pp.267-281, Knoxville, Tennessee, May 1996.

https://doi.org/10.21000/JASMR96010267